SIOC 221A Final Project

Luke Colosi
SIOC 221A: Analysis of Physical Oceanographic Data

June 23, 2020

1 Significant Wave Height and Wind Speed Spectra

Fig. 1 shows the placement of NDBC buoys I choose to conduct my analysis of surface waves and sea surface wind speed relationship in expansion fan regions. Wind Speed (WSP) contour map of boreal summer is displayed to show regional extent of expansion fan winds. Due to WSP being collected by satellite altimetry with $1circ$ by $1circ$ spatial resolution, near shore measurements can possible have land contaminated and therefore maybe unreliable. This could conceivably account for the abrupt drop in WSP several kilometers off the coast of California. The Northern California buoy (station 46014: Point Arena) was chosen for its close proximity to the center of the expansion fan wind event and the Southern California buoy (station 46047: Tanner bank) was chosen because it was outside of the expansion fan wind region. For the Southern Caribbean, there was a limited selection of buoys, however fortunately station 42058 in proximity the coast of Haiti was located in the center of the expansion fan wind region in the Caribbean.

I began my analysis by looking at the raw time series of significant wave height (Hs) and WSP in each region in order to general sense of the variability present in each of the time series and to inspect the time series for gaps and outliers. Fig. 2 shows these time series for each NDBC buoy which spectral and coherence analysis was preformed on. Notice there are gaps present in the some of the time series which are on the order of one or two months. These gaps are not ideal especially when computing spectra and coherence. However, these records were the longest time series of relative continuous data (other segments of these buoys' records contained gaps on the order of a year). by inspecting Fig. 2, we can see an annual cycle present clearly for Hs. However, in the California coast region, WSP has a significant amount of high variability making its annual cycle a less clear. Additionally, the WSP follows a Rayleigh distribution which leads to spikiness in the time series. In the Caribbean, there is a clearer semi-annual cycle present.

In order to obtain a clearer understanding of the annual and semi-annual cycle intraannual variability present in our time series, I computed climatologies for each buoy for Hs and WSP over the time period in Fig. 2. Fig. 3 shows characteristic behavior in the Hs and WSP climatologies in expansion fan region. This characteristic behavior is namely WSP reaching a maximum during the early summer months of June or July and a correspond increase in the Hs climatology at the same time as the WSP maximum. This relationship between the

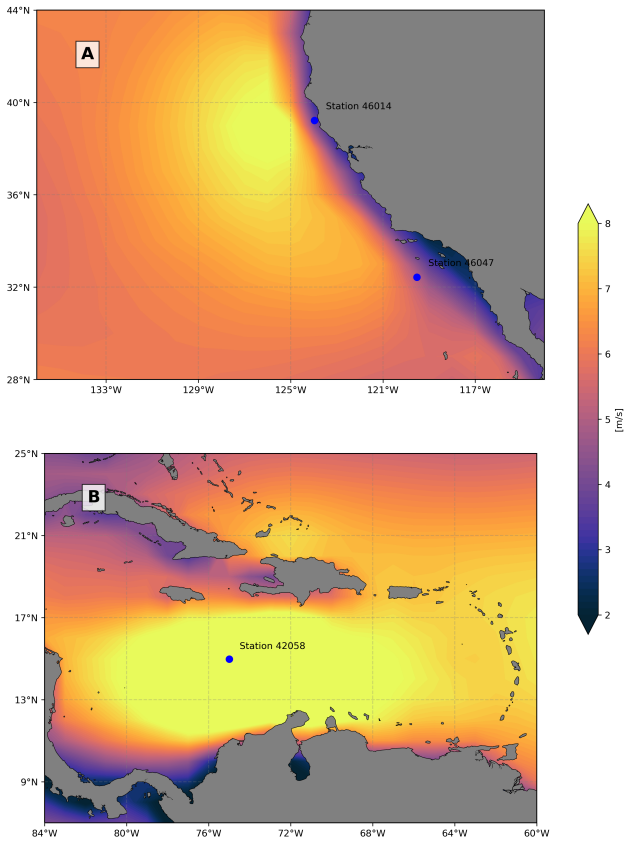

Figure 1: Regional maps of California Coast and Southern Caribbean illustrating NDBC Buoy placement in expansion fan wind regions. Wind Speed contour map of boreal summer (June, July, and August) seasonal average from satellite altimetry product produced by IFREMER shows the general region which characteristic high wind speed occurs from expansion fan winds.

Hs and WSP is indicative of the wave field becoming dominated by locally forced waves (wind sea) during the early summer months which causes a deviation from the annual cycle. The annual cycle is a manifestation of the wave field's primary tendency to be dominated by remotely forced waves (swell) in the California coast region. Additionally, we can obtain a general impression of the phase difference between Hs and WSP at the annual frequency. In expansion fan wind regions, the local wind speed's annual cycle seems to have a phase difference of π from Hs such that Hs annual cycle lags 6 months behind the WSP annual cycle. On the other hand, in the Caribbean, the relationship between Hs and WSP seem to mirror each other very closely such that the phase difference between Hs and WSP is near zero at the annual and semi-annual frequencies. This implies that the waves with the Caribbean are almost exclusively locally forced by the local wind events.

To begin the coherence analysis, I computed power density spectra for each of the NDBC buoy. With the foreknowledge that I would be using these segments for computing spectra in the coherence analysis, I had to choose the time series used for computing spectra such that the annual cycle was accurately resolved (i.e. the time series had to be greater than

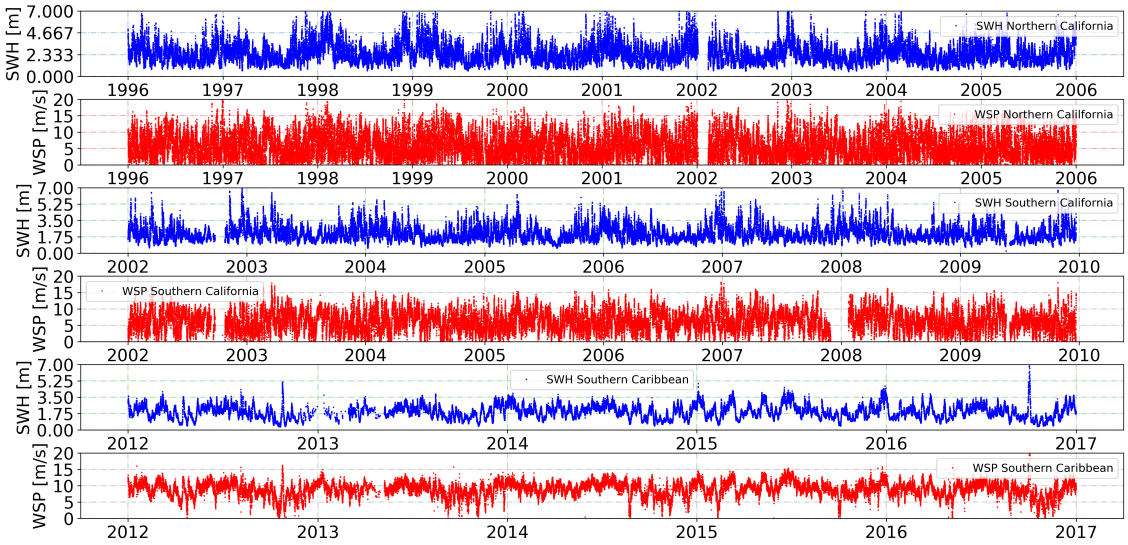

Figure 2: Time series of Hs (meters) and WSP (meters per sec) with hourly sampling rate for NDBC buoys in the regions of Northern California, Southern California, and the Southern Caribbean. Time series are used in spectral and coherence calculations (note daily averaging occurred before spectral and coherence analysis).

1 year long) while still having enough segments to average. After visually inspecting each time series, I decided to use the longest relatively continuous and evenly space record for each buoy without being concerned whether the time record for the buoys were the same length or period. The general methodology of compute the power density spectra consisted of segmenting time series, detrending (removing mean and linear trend), applying a Hanning window, Fourier transforming each segment, computing the squared amplitude of positive frequency Fourier coefficients normalized by N^2 and df, and averaging all segmented spectra to obtain a mean spectral estimate. Additionally, before computing spectra, I averaged the hourly Hs and WSP data to daily resolution in order to remove the high frequency variability which would affect the amount of noise present in the computed spectra. Figs. 4, Fig. 5, and Fig. 6 show the spectra from each NDBC buoy for Hs and WSP using the full time series and segmentation. For Northern and Southern California, there is a clear spectral peak at the annual cycle frequency and a less noticeable peak at the semi-annual frequency for both Hs and WSP (semi-annual peak is less noticeable in Southern California than Northern California for Hs and WSP). Additionally, WSP seems to have a more noticeable semi-annual peak than Hs in Northern California. The spectral slopes are relatively flat, however Hs and WSP are still red spectra at all buoys. For the Southern Caribbean, Hs and WSP mirror each other by having a large spectral peak at both the annual and semi-annual frequencies. For all spectra, Hs has less spectral energy and therefore variability than WSP. Notice that in all my segmented spectra that the annual cycle is not very well resolved (i.e. the spectral peak at the annual frequency is broad. This is slightly problematic in the coherence plots. I had to properly balance resolving the annual cycle per segment while still having enough segments to average between during my coherence analysis.

In order to address this problem of number of segments to spectral resolution of the

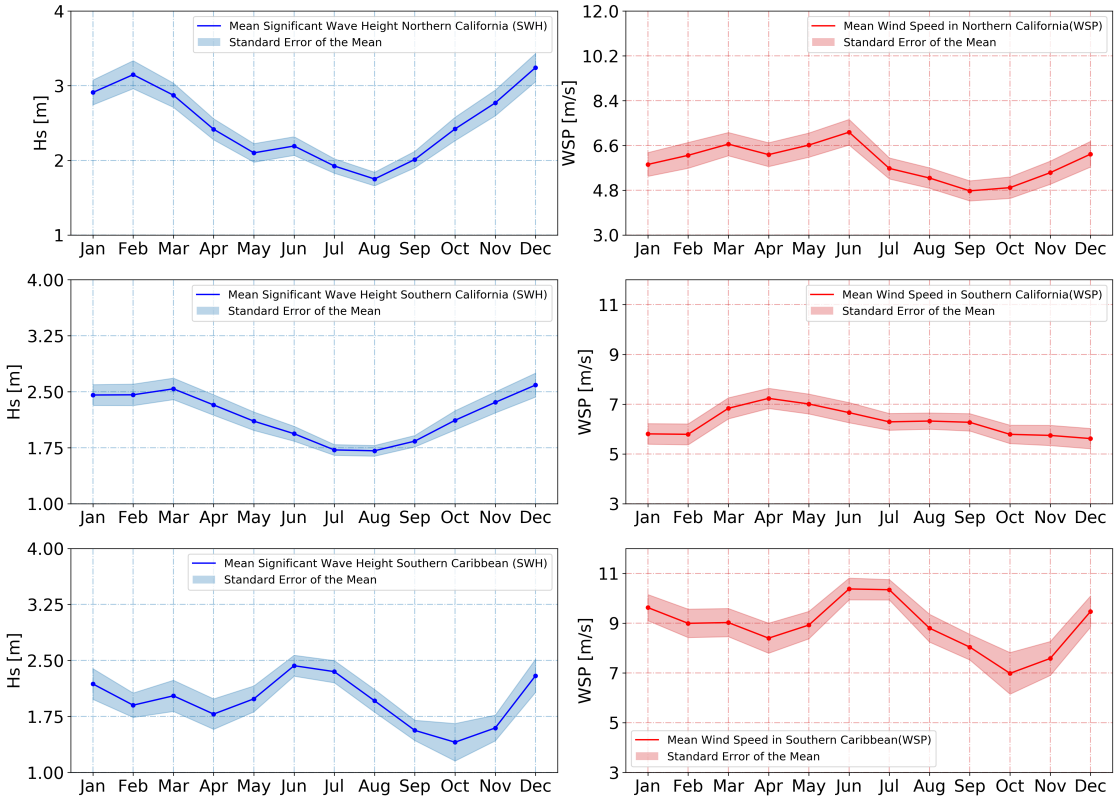

Figure 3: Climatologies of Hs and WSP for NDBC buoys in the regions of Northern California, Southern California, and the Southern Caribbean computed over the time series in Fig. 2 for each buoy. Uncertainty is standard error of the mean with effective number of independent measurements of Hs and WSP computed by finding decorrelation time scales.

annual and semi-annual cycles, I decided to preform the same analysis with modeled CSFR WW3 WSP and Hs data which had longer records of evenly spaced continuous data. The results of extending the time series with the modelled data allowed me to resolve the annual cycle's spectral peak per segment more accurately, and coherence and phase figures obtained more accurate results. Spectral plots from WW3 are included in appendix. Note that CFSR WW3 Hs and WSP obtained from IFREMER has 0.5° by 0.5° spatial resolution and data was chosen for computing spectra was the nearest grid point to buoy location from January 1993 to December 2016.

2 Coherence Analysis

For coherence, I used the Fourier coefficients from the Fourier transformed segmented data (50% overlapping detrended and Hanning windowed segments) from the previous spectra to compute the coherence between Hs and WSP. Fig. 7 shows the coherence between Hs and WSP as a function of cycles per year for each buoy with a 95% significance level threshold per buoy in the top panel. In the bottom panel, Fig.7 shows the phase difference between HS and WSP with standard deviation error bars. For Northern and southern California,

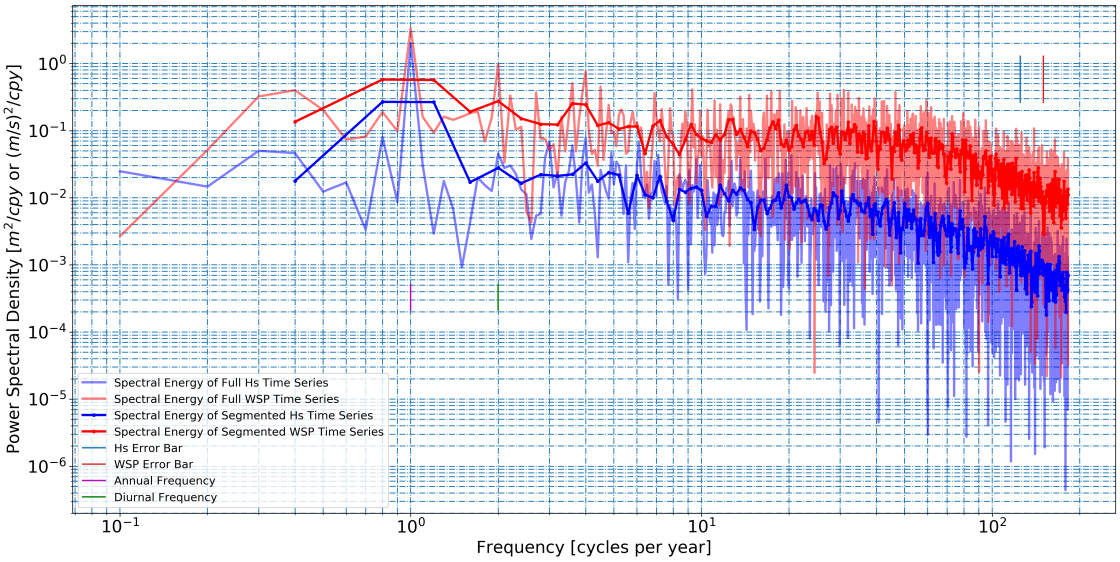

Figure 4: Power density spectra as a function of frequency in cycles per year for Hs (blue curves) and WSP (red curves) at Northern California NDBC buoy with error bars in the top right corner. Time series of daily averaged Hs and WSP extending from January 1st, 1996 to December 31st, 2005 was used to compute the spectra with 9 segments (length of time series per segment is 2.5 year) 50% overlapped (solid curves) and with the full time series (faded curves).

the coherence is significant at the annual and semi-annual frequencies which was expected because the phase relationship between the annual cycles of Hs and WSP should be consistent throughout the time series. The phase difference at the annual cycle is slightly less than -1.5 radians. This is slightly unexpected because I hypothesized based on the climatologies in Fig. 3 that the Hs has approximately a π phase difference from WSP. However, I attribute this to the segments' low resolution of the annual cycle's spectral peak. Additionally, the WSP maximum occurs in the early boreal summer months which would mean that the phase difference would be slightly less than π. Furthermore, the phase difference is negative which implies that Hs lags WSP. This is in agreement with my physical intuition. The semi-annual frequency phase difference is near zero for both Northern and Southern California. Many other frequencies are above the significance level for Northern and Southern California (an amount that I would think would surpass 5% of data). However, the coherence seems to move above and below the 95% significance threshold relatively consistently after the semi-annual frequency which I think would imply that it is insignificant. For the Southern Caribbean, the coherence between Hs and WSP is considered significant for a considerable amount of frequencies. This would be in relative agreement with the fact the Hs and WSP mirror each other very closely through the time series. Focusing on the annual and semi-annual frequencies, the coherence is near unity and the phase difference is near zero. This again agrees with the physical intuition that the wave field is almost exclusively dominated by locally forced wind waves.

By comparing our results from the NDBC buoy coherence plots with the coherence plots from CSFR WW3 Hs and WSP data in Fig. 8, we obtain relatively the same result. However,

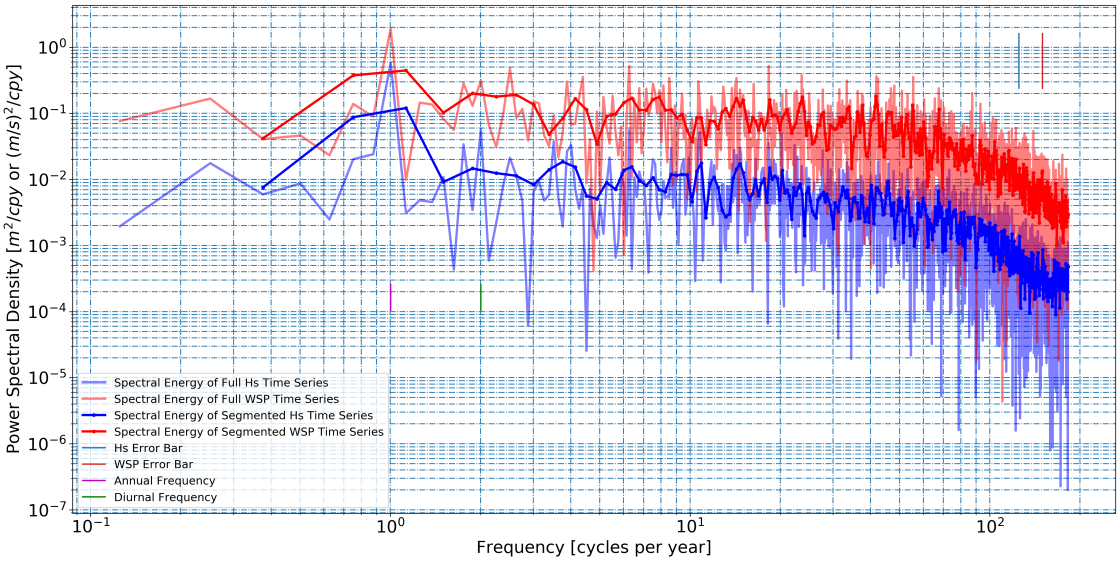

Figure 5: Power density spectra as a function of frequency in cycles per year for Hs (blue curves) and WSP (red curves) at Southern California NDBC buoy with error bars in the top right corner. Time series of daily averaged Hs and WSP in extends from January 1st, 2002 to December 31st, 2009 was used to compute the spectra with 5 segments (length of time series per segment is 2.6 year) 50% overlapped (solid curves) and with the full time series (faded curves).

the longer time series of the CSFR WW3 data allowed me to have more segments which cut down the noise in the coherence plots. Furthermore, the spectral peaks of the annual and semi-annual cycle were resolved much more accurately than for the NDBC data. Therefore, the coherence at the annual and semi-annual cycles was peakier and and the phase differences more accurate. For Northern California, the phase differences between Hs and WSP approached π for the annual frequency and was near zero for the semi annual frequency. For Southern California, the phase difference stayed approximately the same for the annual cycle, but increased to a positive value for the semi-annual cycle. The results were the same for the Southern Caribbean.

Therefore, though the coherence analysis, our understanding of the dynamics in is reinforced such that the expansion fan wind region off the California coast has a nearly out of phase WSP annual cycle compared to the Hs annual cycle. Additionally, the Southern Caribbean has WSP and Hs follow each other extremely closely which again implies that the wave field is dominated by locally forced wind waves.

3 Application of In–situ and Model Data Spectra

Through preforming the spectral and coherence analysis for in-situ and modeled data, I was able to compare the CSFR WW3 model with these in-situ observation. Therefore, we could obtain a sense of how accurate the model is. Through visual inspect of the climatologies and the spectra, the model seems to accurately predict the observations of the buoys with a few

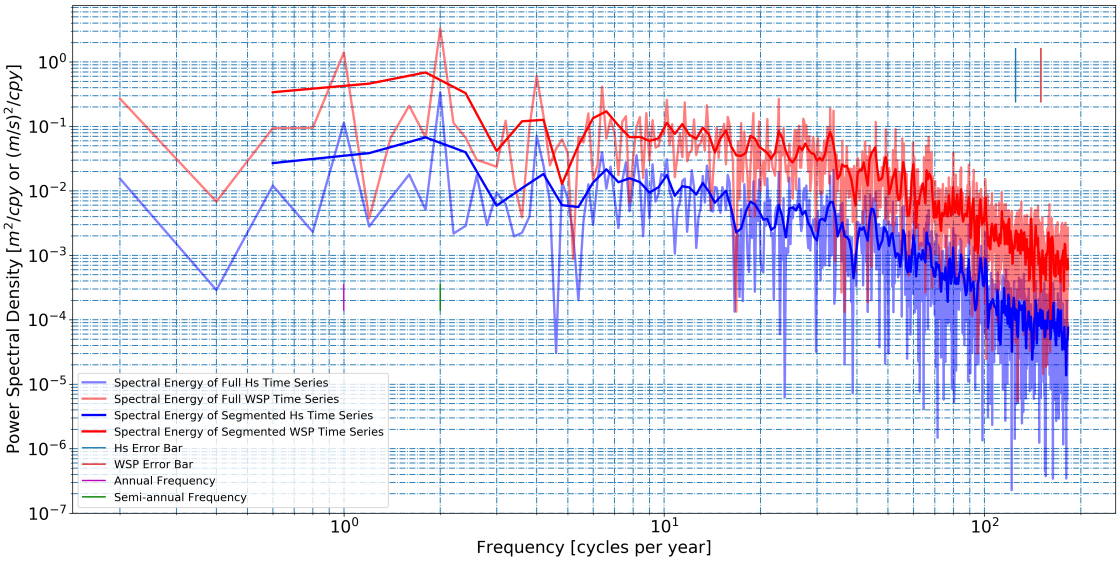

Figure 6: Power density spectra as a function of frequency in cycles per year for Hs (blue curves) and WSP (red curves) at Northern California NDBC buoy with error bars in the top right corner. Time series of daily averaged Hs and WSP in extends from January 1st, 2012 to December 31st, 2016 was used to compute the spectra with 5 segments (length of time series per segment is 1.6 year) 50% overlapped (solid curves) and with the full time series (faded curves).

exceptions. For the climatologies (Fig. 3 and Fig. 9), WSP seems to overestimated WSP in the Caribbean significantely (3 m/s). Additionally, there are many small structures in the buoy climatologies that are captured in the WW3 climatologies. For the spectra of Hs and WSP, the WW3 model seems to have higher energy at the annual and semi-annual spectral peaks than the NDBC buoys.

4 Appendix

Here are additional figures of monthly climatologies and power density spectra from the WW3 model at grid points closest to the location of the buoy.

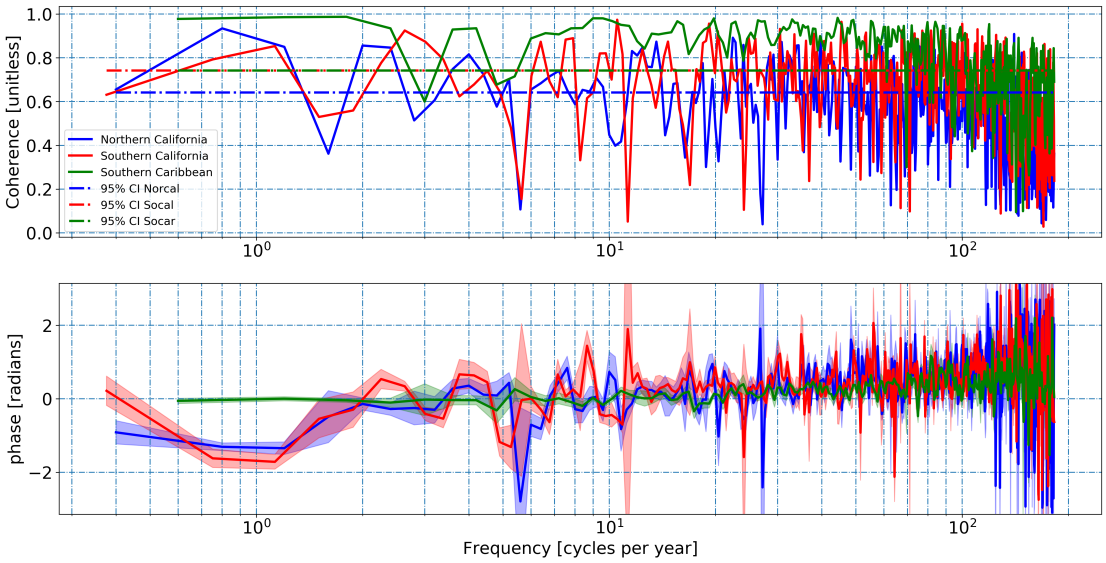

Figure 7: Top panel: Coherence between Hs and WSP as a function of frequency in cycles per year for Northern California (blue curve), Southern California (red curve), and Southern Caribbean (green curve) NDBC buoys with 95% confidence interval for each buoy. Bottom panel: Phase difference between Hs and WSP for each NDBC buoy (same colors) with standard deviation error bars.

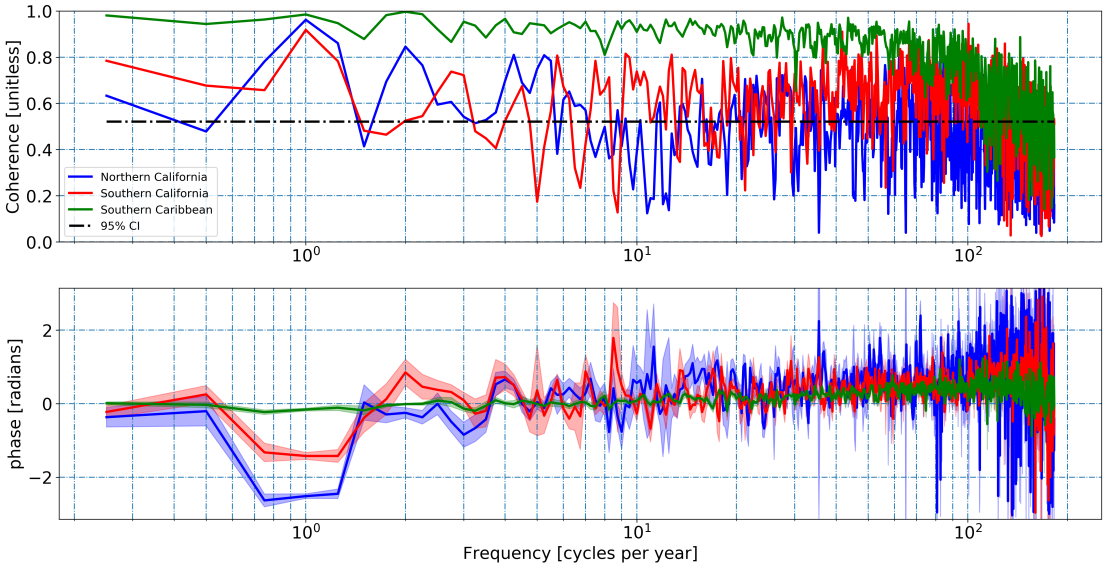

Figure 8: Top panel: Coherence between Hs and WSP as a function of frequency in cycles per year for Northern California (blue curve), Southern California (red curve), and Southern Caribbean (green curve) regional CFSR WW3 data with 95% confidence interval applicable for each coherence function. Bottom panel: Phase difference between Hs and WSP for each region (same colors) with standard deviation error bars.

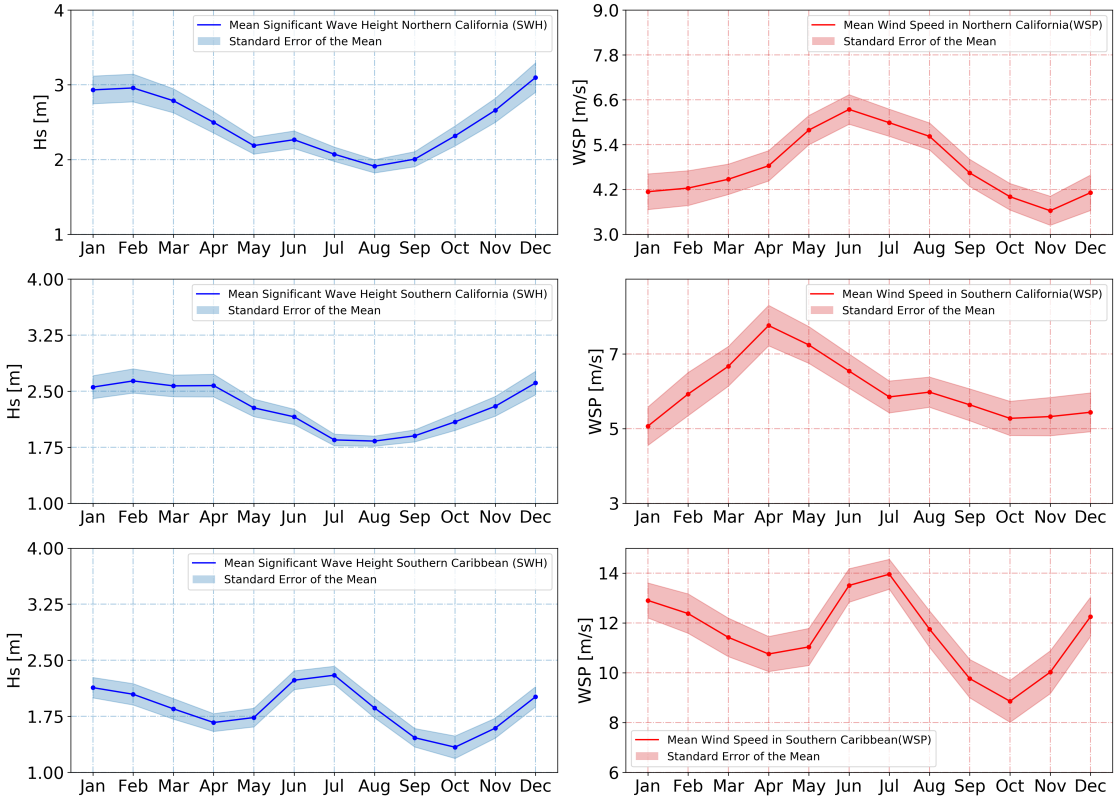

Figure 9: Climatologies of Hs and WSP for CSFR WW3 in the regions of Northern California, Southern California, and the Southern Caribbean computed from January, 1993 to December 2016. Uncertainty is standard error of the mean with effective number of independent measurements of Hs and WSP computed by finding decorrelation time scales.

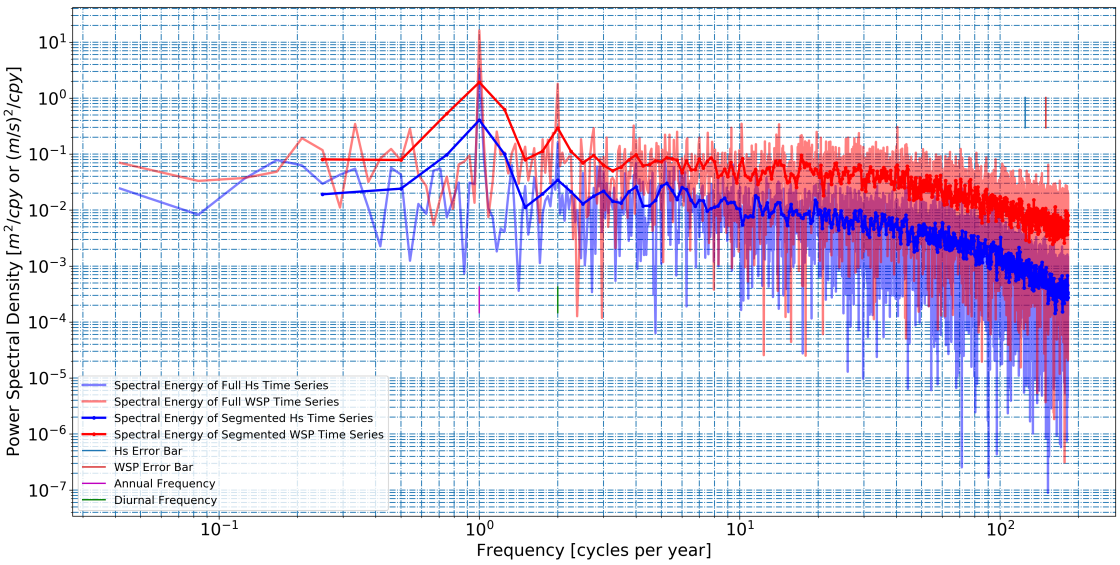

Figure 10: Power density spectra as a function of frequency in cycles per year for Hs (blue curves) and WSP (red curves) in Northern California ($39.0°N$ and $124.0°W$) with error bars in the top right corner. Time series of daily averaged Hs and WSP in extends from January 1st, 1993 to December 31st, 2015 was used to compute the spectra with 15 segments (length of time series per segment is 3 years) 50% overlapped (solid curves) and with the full time series (faded curves).

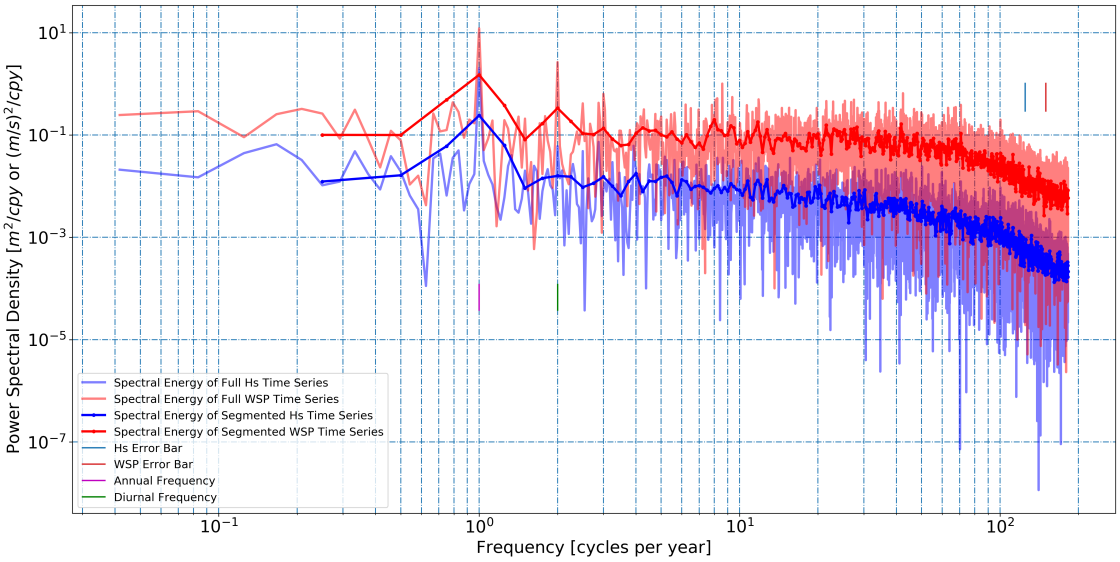

Figure 11: Power density spectra same as Fig. 10 but in the Southern California region ($32.5°N$ and $119.5°W$).

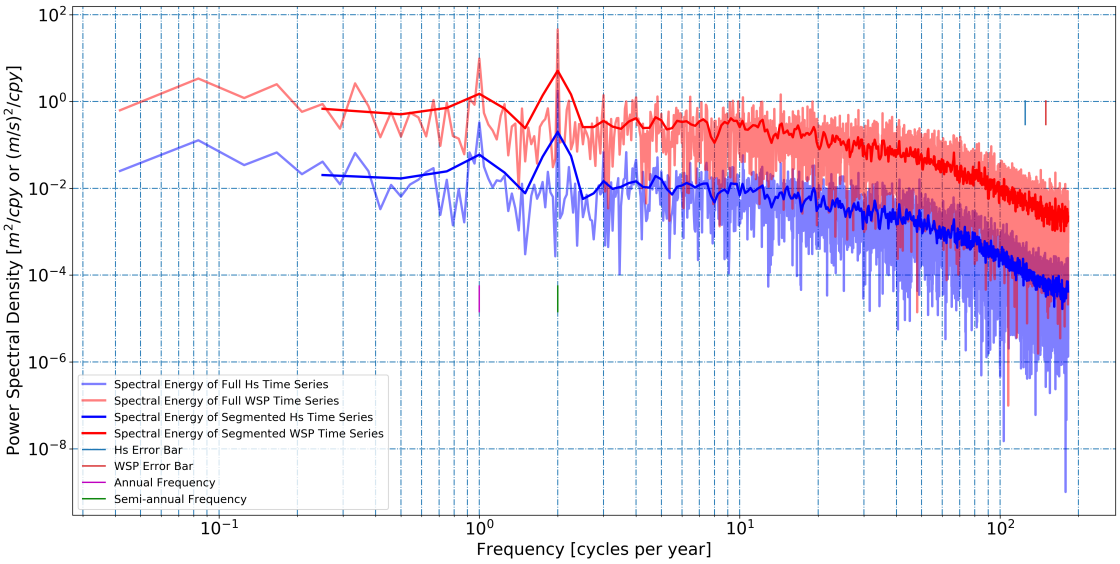

Figure 12: Power density spectra same as Fig. 10 but in the Southern Caribbean region ($15.0°N$ and $75.0°W$).